

# Transparent and Robust Siloxane-Based Hybrid Lamella Film As a Water Vapor Barrier Coating

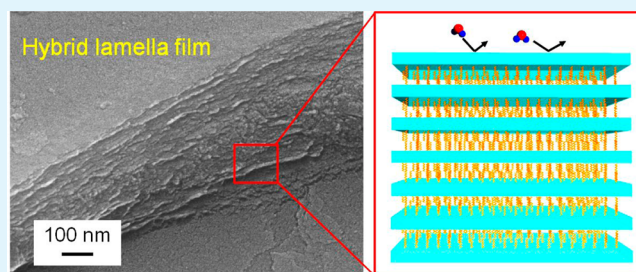
Yasuaki Tokudome,\* Takaaki Hara, Risa Abe, and Masahide Takahashi\*

Department of Materials Science, Graduate School of Engineering, Osaka Prefecture University, Sakai, Osaka 599-8531, Japan

## S Supporting Information

**ABSTRACT:** Water vapor barriers are important in various application fields, such as food packaging and sealants in electronic devices. Polymer/clay composites are well-studied water vapor barrier materials, but their transparency and mechanical strength degrade with increasing clay loading. Herein, we demonstrate films with good water vapor barrier properties, high transparency, and mechanical/thermal stability. Water vapor barrier films were prepared by the solution crystallization of siloxane hybrid lamellae. The films consist of highly crystallized organic/inorganic hybrid lamellae, which provide high transparency, hardness, and thermal stability and inhibit the permeation of water vapor. The water permeability of a 6  $\mu\text{m}$  thick hybrid film is comparable to that of a 200  $\mu\text{m}$  thick silicon rubber film.

**KEYWORDS:** gas barrier film, hybrid film, lamella, water vapor transmission rate, sol-gel



## INTRODUCTION

Controlling gas permeation through materials is a key technological issue in gas separation and storage, protective coatings, and packaging.<sup>1–4</sup> Water vapor barriers are considerably important in food packaging,<sup>5–7</sup> sealants in light-emitting diodes,<sup>8,9</sup> and biomedical implants.<sup>10</sup> One challenge for advanced water barrier materials is simultaneously achieving high light transmittance, thermal/mechanical stability, flexibility, and good water barrier property. Organic–inorganic hybrids can potentially meet these requirements. Polymer/clay hybrid films such as polylactide/montmorillonite have received much interest as water barrier materials over a few decades.<sup>11–14</sup> These hybrids involve inorganic clays being melt-blended with polymers to give polymer/clay hybrid composites containing <10 wt % clay.<sup>15,16</sup> High aspect ratio clay plates inhibit the permeation of water vapor by providing a high effective diffusion length. This is known as the tortuous pathway concept<sup>17</sup> and is applicable to various polymer/clay combinations.<sup>18</sup>

The water barrier properties of polymer/clay hybrid films are theoretically enhanced with increasing the dimension and volume fraction of the incorporated clay.<sup>19</sup> However, their light transparency and mechanical strength degrade with increasing clay loading. For example, the tensile strength of polymer/clay hybrid films reportedly increases with increasing filler (montmorillonite) concentration up to 3 wt %, after which it decreases sharply due to aggregation within the matrix.<sup>16,20</sup> Overcoming this trade-off between good water vapor barrier properties and optical/physical properties remains a challenge.

Herein, we report a novel strategy for films with good water vapor barrier properties, high transparency, and mechanical/thermal stability. Water vapor barrier films were prepared by

the solution crystallization of siloxane hybrid lamellae; siloxane hybrid lamellae are crystallized within coated films upon drying. The lamellae form homogeneous films, despite the high crystallinity of the film (lamella loading >48% by volume). The highly crystallized organic/inorganic hybrid lamellae provide high transparency, hardness, and thermal stability. Moreover, the hybrid lamellae successfully work as “clays” and inhibit water permeation through the film. The water permeability of a 6  $\mu\text{m}$  thick hybrid film is comparable to that of a 200  $\mu\text{m}$  thick silicon rubber film. The siloxane-based barrier film has potential in various applications; silicone rubber is a medically approved bio-inert sealing material, though its water barrier properties have not yet reached acceptable levels.<sup>21</sup> The water vapor transmission rate (WVTR) of the hybrid lamellar film is comparable to that of poly-L-lactide and polyurethane films widely used in food packaging ( $10^1$ – $10^2$   $\text{g}\cdot\text{m}^{-2}\cdot\text{d}^{-1}$  at a film thickness of 100  $\mu\text{m}$ ).<sup>1,14,22</sup> In-situ crystallized lamellae can therefore impart siloxane-based materials with water barrier properties.

## EXPERIMENTAL METHODS

**Synthesis of Hybrid Films with Lamellar Structures.** The synthesis was based on reported syntheses of crystalline hybrid silicates.<sup>23,24</sup> Trimethoxy(7-octen-1-yl)silane (TM7O1S, 80%; Sigma-Aldrich Corp., St. Louis, MO), tetramethyl orthosilicate (TMOS; Shin-Etsu Chemicals Co., Ltd., Japan), hydrochloric acid (HCl, 36 wt % in  $\text{H}_2\text{O}$ ; Wako Pure Chemicals Industries, Ltd., Japan), ultrapure water, and tetrahydrofuran (THF,  $\geq 99.5\%$ ; Wako Pure Chemicals Industries, Ltd., Japan) were mixed at a TM7O1S/TMOS/HCl/ $\text{H}_2\text{O}$ /

Received: August 13, 2014

Accepted: October 7, 2014

Published: October 8, 2014

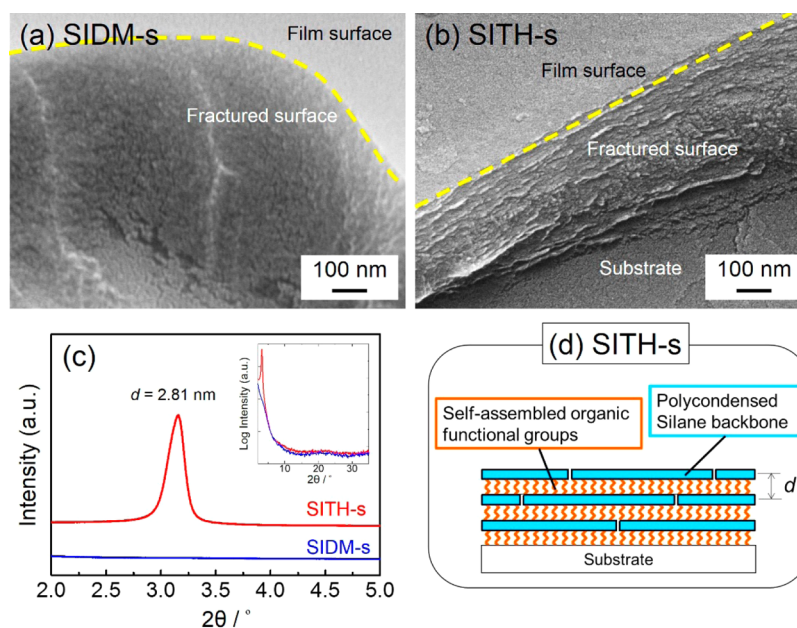


**Figure 1.** SEM images of (a) SIDM-s and (b) SITH-s; yellow dotted lines show the interface between the surface and interior. (c) Out-of-plane XRD patterns of SITH-s and SIDM-s. (d) Schematic showing the oriented hybrid lamellae of SITH-s.

THF molar ratio of  $1:4:2 \times 10^{-3}:28.5:15$ . The mixture was stirred for 10 h at room temperature and then diluted with THF to achieve a TM7O1S/THF ratio of 1:40. The solution was spin-coated onto a 30  $\mu\text{m}$  thick pre-cleaned Cu substrate (#CU-113243, Nilaco Corp., Japan) at 25  $^{\circ}\text{C}$ , 45% relative humidity, and a spinning rate of 1000 rpm for 30 s. Prior to coating, the Cu substrate was ultrasonically cleaned in acetone for 20 min. The film was aged for 12 h in a closed container containing silica gel and a deoxygenator (Sequel, Nisso Fine Co., Ltd.). The film was irradiated with UV light ( $\lambda = 254 \text{ nm}$ ,  $10 \mu\text{W}/\text{cm}^2$ ) for 12 h in a  $\text{N}_2$  atmosphere to achieve the cross-linking of  $\text{C}=\text{C}$  bonds in TM7O1S.<sup>24</sup> The obtained hybrid film was named SITH-s, where s denotes a single coating. The above procedure was repeated to achieve a multilayer coating named SITH-m, where m denotes a multilayer coating. The number of layers in the coating was  $\leq 10$ . For comparison, another hybrid film was prepared from a mixed solvent. An identical composition (TM7O1S/TMOS/HCl/ $\text{H}_2\text{O}$ /THF =  $1:4:2 \times 10^{-3}:28.5:15$ ) was stirred for 10 h and then diluted with THF and *N,N*-dimethylformamide (DMF,  $\geq 99.5\%$ ; Wako Pure Chemicals Industries, Ltd., Japan) to achieve a TM7O1S/THF/DMF ratio of 1:30:10. The procedure was then continued as for SITH-s. The resulting film was named SIDM-s. The film surface was processed in an UV/ $\text{O}_3$  chamber (ASM1101N, Asumi Giken, Ltd.) for 1 min before repeating the procedure to yield a film with multilayer coating, SIDM-m.

**Characterization.** Field emission scanning electron microscopy (FE-SEM; S-4800, Hitachi, Japan, Pt/Pd coating) was used to observe the layered structures of films. Crystallinities of films were investigated by X-ray diffraction (XRD; SmartLab, Rigaku, Tokyo, Japan), using  $\text{Cu K}\alpha$  radiation ( $\lambda = 0.154 \text{ nm}$ ). UV-visible (UV-vis) spectrophotometry (V-670, JASCO Corp.) was used to measure the transmittance of films coated on silica glass substrates. A bare silica glass substrate was used as the reference. The thickness of the film was measured by laser scanning confocal microscopy (LSCM; SFT23500, Shimadzu Corp.). Thermogravimetric analysis (TGA; Thermo Plus Evo, Rigaku, Japan) was carried out for the hybrid films cast on polytetrafluoroethylene sheets and subjected to UV irradiation. Analysis was conducted at a heating rate of 3  $^{\circ}\text{C}/\text{min}$  in a  $\text{N}_2$  atmosphere. The pencil hardness of 1  $\mu\text{m}$  thick films coated on soda-lime-glass substrates was measured using a 750 g loading in at least three locations. The scratch rate and distance were 0.5 mm/s and  $\sim 1 \text{ cm}$ , respectively.

**Measurement of Water Barrier Properties.** The film supported on a Cu substrate was placed on a 100  $\mu\text{m}$  thick silicone rubber sheet (#244-6012-02, ARAM Corp.), and immersed in 37.5 wt % aqueous  $\text{FeCl}_3$  (Wako Pure Chemicals Industries, Ltd., Japan). The Cu substrate was etched after a given duration, and the hybrid film transferred to the silicon rubber sheet. The hybrid film on the silicone rubber sheet was kept at room temperature with a desiccant, and its water barrier properties were investigated. The WVTR ( $\text{g}\cdot\text{m}^{-2}\cdot\text{d}^{-1}$ ) was evaluated using a purpose-built apparatus, according to Japanese Industrial Standard No. Z0208-1976 (Figure S1, Supporting Information).

## RESULTS AND DISCUSSION

The SITH-s and SIDM-s films had comparable thicknesses of  $\sim 400 \text{ nm}$ . Pinholes within films can degrade their water vapor barrier properties, and these were not observed by SEM. In Figure 1, panels a and b show SEM images of cross sections of fractured SIDM-s and SITH-s films, respectively. The nanostructure of SIDM-s composed of aggregated particles 10–20 nm in diameter (Figure 1a). SITH-s had a layered nanostructure consisting of lamella plates of 10–20 nm in thickness and 100–300 nm in width (Figure 1b and Figure S2, Supporting Information). The XRD patterns of the samples indicated that their different nanostructures were derived from their structure ordering (Figure 1c). SIDM-s had a disordered nanostructure, whereas SITH-s had a lamellar nanostructure, as confirmed by the XRD peak at  $3.2^{\circ}$ . The difference of ordering reportedly originates from different evaporation rates of DMF and THF. Relatively slow evaporation of DMF induces extensive condensation of Si alkoxides to prevent ordering of lamellae.<sup>25</sup> The  $d$  value of the XRD peak for SITH-s was 2.8 nm, which suggested that organic groups were arranged in a zip-like manner. The head-to-head bimolecular packing of octyltrialkoxysilane reportedly produced lamellae with a  $d$  spacing of  $> 3 \text{ nm}$ .<sup>26</sup> The hybrid lamellae within the SITH-s film were strongly orientated. A sharp peak originating from the hybrid lamellae was detected in the XRD pattern recorded in an out-of-plane geometry but was not detected in the pattern recorded in-plane (Figure S3, Supporting Information). Thus,

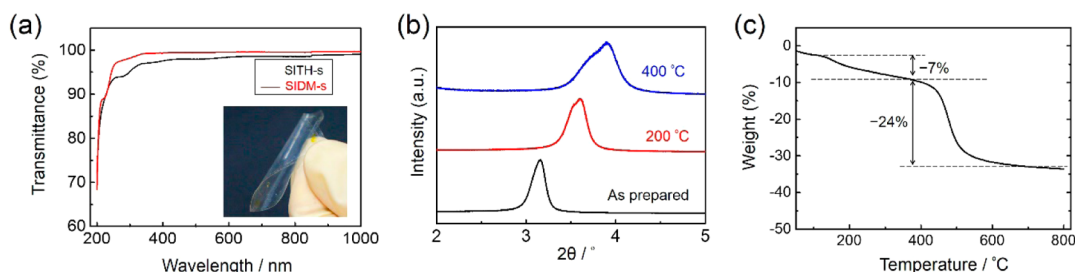


**Figure 2.** (a) UV-vis absorption spectra of (black) SITH-s and (red) SIDM-s; (inset) SITH-m supported on a silicone substrate. (b) XRD patterns of SITH-s after being subjected to heat treatment at various temperatures for 1 h. (c) TGA curve of the hybrid siloxane cast film.

the hybrid lamellae were ordered on the substrate, as shown in Figure 1d. The high crystallinity of the SITH-s film was apparent from the SEM image (Figure 1b and Figure S2, [Supporting Information]), and the high peak intensity in the XRD pattern (Figure 1c).

The hybrid films containing lamella crystals possessed attractive physical and chemical properties. SITH-s exhibited a transparency of 98% at 550 nm (Figure 2a), which was comparable to SIDM-s with an amorphous structure. SITH-s was polycrystalline and highly transparent, because of the stacking of lamellar hybrid plates without aggregation. The flexibility and transparency of the film is shown in the photo inset in Figure 2a. Homogeneous transparent films with hybrid lamellas would allow the tuning of optical properties, such as refractive index and optical anisotropy.<sup>27</sup> Although dispersing clays into the polymers is known to be effective to improve the water barrier property,<sup>11–14</sup> incorporating Laponite into the present siloxane materials resulted in inhomogeneous and translucent films (Figure S4, Supporting Information). SITH-s was thermally stable at temperatures up to 400 °C (Figure 2b). The XRD diffraction peak shifted to a higher angle and broadened slightly with increasing temperature. This was attributed largely to the condensation of unreacted silanols or ethoxy groups in the inorganic backbone, as supported by the 7% weight loss at 400 °C (Figure 2c). The decomposition of organic groups was restricted until 400 °C. The second weight loss of 24% at above 400 °C correlated with the calculated 23.7% weight loss of organic moieties. SITH-s exhibited a high pencil hardness of 6H, in comparison with the amorphous state (5H). The relatively high pencil hardness was due to the oriented crystal plates (100–300 nm in the lateral direction), as shown in Figure 1b. SITH-s possessed high transparency, hardness, thermal stability, and crystallinity. The film thickness could be increased by successive coatings up to  $\sim 6 \mu\text{m}$ , above which cracks formed upon drying. A further increase of film thickness is possible by optimizing the thermal annealing process of the film at respective coating steps.<sup>28,29</sup> The present hybrid films can be bound together with a siloxane-based glue owing to chemically bondable silanols on their surfaces, which potentially allows to produce thick films.

Figure 3 shows the WVTR values of SITH-m, SIDM-m, and commercial silicone. WVTR measurements were performed on samples on 100  $\mu\text{m}$  thick silicon rubber substrates; therefore, both the sample film and rubber substrate contributed to the WVTR. SIDM-m with an amorphous structure exhibited a constant WVTR with increasing film thickness. SITH-m containing hybrid lamellae exhibited a decreasing WVTR with increasing film thickness. At any given film thickness, SITH-m had a much lower WVTR than SIDM-m. SITH-m and SIDM-m had identical chemical compositions, so their differing

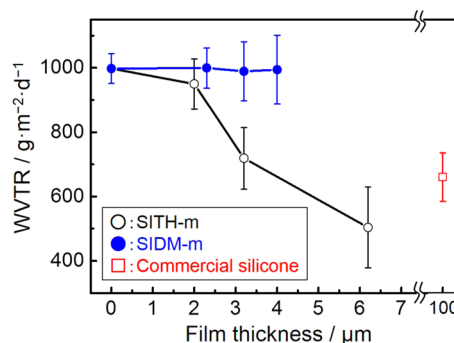


**Figure 3.** WVTR values with increasing film thickness for SITH-m, SIDM-m, and 100  $\mu\text{m}$  thick commercial silicone. The film thickness of SIDM-m was  $< 4 \mu\text{m}$  because cracks formed during the coating of thicker films. Measurements were performed on SITH-m and SIDM-m films on 100  $\mu\text{m}$  thick silicone rubber substrates. The WVTR of commercial silicone was measured on another silicone rubber substrate, which enabled its comparison with SITH-m and SIDM-m.

WVTR values were due to their differing nanostructures. The ordered hybrid lamellae inhibited the permeation of water through the film. Water permeation through 6.2  $\mu\text{m}$  thick SITH-m was lower than that through 100  $\mu\text{m}$  thick commercial silicone. The WVTR values of self-standing films (i.e., not supported on rubber substrates) were calculated from the results in Figure 3 using Fick's first law. The calculated WVTR values of self-standing SITH-m (ss-SITH-m) films were  $2.2 \times 10^4$ ,  $2.6 \times 10^3$ , and  $1.0 \times 10^3 \text{ g}\cdot\text{m}^{-2}\cdot\text{d}^{-1}$  for film thicknesses of 2.0, 3.2, and 6.2  $\mu\text{m}$ , respectively. The WVTR of self-standing SIDM-m (ss-SIDM-m) was not easily calculated, because of its negligible water vapor barrier properties. The WVTR of 4  $\mu\text{m}$  thick ss-SIDM-m was estimated to be no lower than  $10^4 \text{ g}\cdot\text{m}^{-2}\cdot\text{d}^{-1}$ . The calculated WVTR of 100  $\mu\text{m}$  thick ss-SITH-m was  $63 \text{ g}\cdot\text{m}^{-2}\cdot\text{d}^{-1}$ , which was 30 times smaller than a silicone rubber film of the same thickness. At a thickness of 100  $\mu\text{m}$ , the WVTR of  $63 \text{ g}\cdot\text{m}^{-2}\cdot\text{d}^{-1}$  is comparable to those of poly-L-lactide<sup>1</sup> (PLA;  $10^1$ – $10^2 \text{ g}\cdot\text{m}^{-2}\cdot\text{d}^{-1}$ ) and polyurethane<sup>22</sup> (PU;  $\sim 20 \text{ g}\cdot\text{m}^{-2}\cdot\text{d}^{-1}$ ), and larger than those of polyethylene<sup>30</sup> ( $\sim 3 \times 10^{-1} \text{ g}\cdot\text{m}^{-2}\cdot\text{d}^{-1}$ ) and polypropylene<sup>30,31</sup> ( $\sim 1 \text{ g}\cdot\text{m}^{-2}\cdot\text{d}^{-1}$ ). These polymers are widely used as packaging materials. The siloxane-based hybrids demonstrated here provide additional advantages of high mechanical/thermal stabilities and bioinertness, which enable their use under severe conditions and for biomedical applications.

The restricted water permeability in SITH-m could be explained by the tortuous pathway concept, which is commonly reported in polymer/clay systems.<sup>32</sup> The water vapor barrier in polymer/clay composites can be described by the Nielsen model.<sup>17</sup>

$$P/P_0 = (1 - \varphi)/(1 + \alpha\varphi/2) \quad (1)$$

where  $P$  is the permeability coefficient of the polymer/clay composite,  $P_0$  is the permeability coefficient of the polymer,  $\varphi$  is the volume fraction of clay (vol %), and  $\alpha$  is the aspect ratio of clay.<sup>32</sup> The lamella crystals possessed a higher density and lower free volume than the corresponding amorphous hybrid siloxane. Thus, the lamellae could be considered as clay within the film. An  $\alpha$  of 10 (estimated from the SEM image in Figure 1b) and  $P/P_0$  calculated from the WVTR values and film thicknesses of SITH-m and SIDM-m yielded a  $\varphi$  of >48%. This was the minimum  $\varphi$  because a WVTR for SIDM-m of  $10^4 \text{ g}\cdot\text{m}^{-2}\cdot\text{d}^{-1}$  was used for the calculation. A  $\varphi$  of  $\geq 48\%$  is much higher than typical clay/polymer systems (<10%), and this high-volume fraction was responsible for the water barrier properties of SITH-m. The high crystallinity and preferential orientation of the lamella overcame the usual trade-off between water vapor barrier properties and transparency and stability. The present liquid phase process is simple and versatile compared with vapor-phase coating techniques<sup>7,33</sup> and is applicable for coating on Cu, Si, glass, polyvinylpyrrolidone, and polycarbonate.

## CONCLUSION

Siloxane-based hybrid lamellar films were prepared by sol-gel reaction. The ordered hybrid lamellae inhibited the permeation of water through the composite film. The WVTR of a  $6.2 \mu\text{m}$  thick lamellar film was  $1.0 \times 10^3 \text{ g}\cdot\text{m}^{-2}\cdot\text{d}^{-1}$ , which was 30 times higher than that of commercial silicone ( $1.8 \times 10^3 \text{ g}\cdot\text{m}^{-2}\cdot\text{d}^{-1}$ ), and comparable to PLA ( $10^1\text{--}10^2 \text{ g}\cdot\text{m}^{-2}\cdot\text{d}^{-1}$ ) and PU ( $\sim 20 \text{ g}\cdot\text{m}^{-2}\cdot\text{d}^{-1}$ ) films widely investigated for food packaging. The hybrid lamellar film exhibited a transparency of 98%, stability at  $400 \text{ }^\circ\text{C}$ , and a scratch hardness of 6H. The present concept can yield highly transparent and stable water vapor barrier films. The concept of using in situ crystallized lamellae can impart siloxane-based materials with high water barrier properties.

## ASSOCIATED CONTENT

### Supporting Information

Detailed description of the WVTR measurement setup and out-of-plane and in-plane XRD patterns. This material is available free of charge via the Internet at <http://pubs.acs.org>.

## AUTHOR INFORMATION

### Corresponding Authors

\*E-mail: tokudome@photomater.com.

\*E-mail: masa@photomater.com.

### Author Contributions

These authors contributed equally.

### Notes

The authors declare no competing financial interest.

## ACKNOWLEDGMENTS

This study was supported by a Grant-in-Aid for Scientific Research (B) (No. 26288108) and a Grant-in-Aid for Challenging Exploratory Research (No. 26630322) from the Ministry of Education, Culture, Sports, Science, and Technology, administrated by the Japan Society for the Promotion of Science. Y.T. acknowledges financial support from The Kazuchika Okura Memorial Foundation. This work was supported by the Hosokawa Powder Technology Foundation.

We thank Drs. Y. Kubota, T. Ide, and M. Seino of Central Glass Co., Ltd., for pencil hardness and water vapor barrier tests.

## REFERENCES

- (1) Tsuji, H.; Tsuruno, T. Water Vapor Permeability of Poly(L-lactide)/Poly(D-lactide) Stereocomplexes. *Macromol. Mater. Eng.* **2010**, *295* (8), 709–715.
- (2) Millward, A. R.; Yaghi, O. M. Metal-Organic Frameworks with Exceptionally High Capacity for Storage of Carbon Dioxide at Room Temperature. *J. Am. Chem. Soc.* **2005**, *127* (51), 17998–17999.
- (3) Stern, S. A. Polymers for Gas Separations: The Next Decade. *J. Membr. Sci.* **1994**, *94*, 1–65.
- (4) Chatham, H. Oxygen Diffusion Barrier Properties of Transparent Oxide Coatings on Polymeric Substrates. *Surf. Coat. Technol.* **1996**, *78* (1–3), 1–9.
- (5) Yang, L.; Paulson, A. T. Effects of Lipids on Mechanical and Moisture Barrier Properties of Edible Gellan Film. *Food Res. Int.* **2000**, *33* (7), 571–578.
- (6) Park, H. J.; Chinnan, M. S. Gas and Water-Vapor Barrier Properties of Edible Films from Protein and Cellulosic Materials. *J. Food Eng.* **1995**, *25* (4), 497–507.
- (7) Hirvikorpi, T.; Vaha-Nissi, M.; Mustonen, T.; Iiskola, E.; Karppinen, M. Atomic Layer Deposited Aluminum Oxide Barrier Coatings for Packaging Materials. *Thin. Solid Films* **2010**, *518* (10), 2654–2658.
- (8) Weaver, M. S.; Michalski, L. A.; Rajan, K.; Rothman, M. A.; Silvernail, J. A.; Brown, J. J.; Burrows, P. E.; Graff, G. L.; Gross, M. E.; Martin, P. M.; Hall, M.; Mast, E.; Bonham, C.; Bennett, W.; Zumhoff, M. Organic Light-Emitting Devices with Extended Operating Lifetimes on Plastic Substrates. *Appl. Phys. Lett.* **2002**, *81* (16), 2929–2931.
- (9) Graff, G. L.; Williford, R. E.; Burrows, P. E. Mechanisms of Vapor Permeation Through Multilayer Barrier Films: Lag Time Versus Equilibrium Permeation. *J. Appl. Phys.* **2004**, *96* (4), 1840–1849.
- (10) Hogg, A.; Uhl, S.; Feuvrier, F.; Girardet, Y.; Graf, B.; Aellen, T.; Keppner, H.; Tardy, Y.; Burger, J. Protective Multilayer Packaging for Long-Term Implantable Medical Devices. *Surf. Coat. Technol.* **2014**, *256*, 124–129.
- (11) Thellen, C.; Orroth, C.; Froio, D.; Ziegler, D.; Lucciarini, J.; Farrell, R.; D'Souza, N. A.; Ratto, J. A. Influence of Montmorillonite Layered Silicate on Plasticized Poly(L-lactide) Blown Films. *Polymer* **2005**, *46* (25), 11716–11727.
- (12) Tenn, N.; Follain, N.; Soulestin, J.; Cretois, R.; Bourbigot, S.; Marais, S. Effect of Nanoclay Hydration on Barrier Properties of PLA/Montmorillonite Based Nanocomposites. *J. Phys. Chem. C* **2013**, *117* (23), 12117–12135.
- (13) Pavlidou, S.; Papaspyrides, C. D. A Review on Polymer-Layered Silicate Nanocomposites. *Prog. Polym. Sci.* **2008**, *33* (12), 1119–1198.
- (14) Auras, R.; Harte, B.; Selke, S. An Overview of Poly(lactides) as Packaging Materials. *Macromol. Biosci.* **2004**, *4* (9), 835–864.
- (15) Liu, R.; Cao, J. Z.; Luo, S. P.; Wang, X. Effects of Two Types of Clay on Physical and Mechanical Properties of Poly(lactic acid)/Wood Flour Composites at Various Wood Flour Contents. *J. Appl. Polym. Sci.* **2013**, *127* (4), 2566–2573.
- (16) Kontou, E.; Niaounakis, M.; Georgiopoulos, P. Comparative Study of PLA Nanocomposites Reinforced with Clay and Silica Nanofillers and Their Mixtures. *J. Appl. Polym. Sci.* **2011**, *122* (3), 1519–1529.
- (17) Nielsen, L. E. Models for the Permeability of Filled Polymer Systems. *J. Macromol. Sci., Part A: Pure Appl. Chem.* **1967**, *1* (5), 929–942.
- (18) Alexandre, M.; Dubois, P. Polymer-Layered Silicate Nanocomposites: Preparation, Properties and Uses of a New Class of Materials. *Mater. Sci. Eng., R* **2000**, *28* (1–2), 1–63.
- (19) Xu, B.; Zheng, Q.; Song, Y. H.; Shangguan, Y. Calculating Barrier Properties of Polymer/Clay Nanocomposites: Effects of Clay Layers. *Polymer* **2006**, *47* (8), 2904–2910.
- (20) Jiang, L.; Zhang, J. W.; Wolcott, M. P. Comparison of Poly(lactide)/Nano-Sized Calcium Carbonate and Poly(lactide)/Mont-

morillonite Composites: Reinforcing Effects and Toughening Mechanisms. *Polymer* **2007**, *48* (26), 7632–7644.

(21) Wasikiewicz, J. M.; Roohpour, N.; Paul, D.; Grahn, M.; Ateh, D.; Rehman, I.; Vadgama, P. Polymeric Barrier Membranes for Device Packaging, Diffusive Control and Biocompatibility. *Appl. Surf. Sci.* **2008**, *255* (2), 340–343.

(22) Osman, M. A.; Mittal, V.; Morbidelli, M.; Suter, U. W. Polyurethane Adhesive Nanocomposites as Gas Permeation Barrier. *Macromolecules* **2003**, *36* (26), 9851–9858.

(23) Shimojima, A.; Wu, C. W.; Kuroda, K. Structure and Properties of Multilayered Siloxane-Organic Hybrid Films Prepared Using Long-Chain Organotrialkoxysilanes Containing C=C Double Bonds. *J. Mater. Chem.* **2007**, *17* (7), 658–663.

(24) Shimojima, A.; Kuroda, K. Novel Layered Silica/Organic Polymer Hybrid Films with the Interface Linked by Si-C Bonds. *Chem. Lett.* **2000**, *11*, 1310–1311.

(25) Shimojima, A.; Sugahara, Y.; Kuroda, K. Synthesis of Oriented Inorganic–Organic Nanocomposite Films from Alkyltrialkoxysilane–Tetraalkoxysilane Mixtures. *J. Am. Chem. Soc.* **1998**, *120* (18), 4528–4529.

(26) Shimojima, A.; Kuroda, K. Structural Control of Multilayered Inorganic–Organic Hybrids Derived from Mixtures of Alkyltriethoxysilane and Tetraethoxysilane. *Langmuir* **2002**, *18* (4), 1144–1149.

(27) Takahashi, M.; Figus, C.; Kichob, T.; Enzo, S.; Casula, M.; Valentini, M.; Innocenzi, P. Self-Organized Nanocrystalline Organosilicates in Organic-Inorganic Hybrid Films. *Adv. Mater.* **2009**, *21* (17), 1732–1736.

(28) Kozuka, H.; Takenaka, S.; Tokita, H.; Okubayashi, M. PVP-Assisted Sol–Gel Deposition of Single Layer Ferroelectric Thin Films over Submicron or Micron in Thickness. *J. Eur. Ceram. Soc.* **2004**, *24* (6), 1585–1588.

(29) Brinker, C. J.; Scherer, G. W. *Sol–Gel Science: The Physics and Chemistry of Sol–Gel Processing*; Academic Press: Boston, 1990.

(30) Garcia, M. A.; Pinotti, A.; Martino, M. N.; Zaritzky, N. E. Characterization of Composite Hydrocolloid Films. *Carbohydr. Polym.* **2004**, *56* (3), 339–345.

(31) Metz, S. J.; van de Ven, W. J. C.; Potreck, J.; Mulder, M. H. V.; Wessling, M. Transport of Water Vapor and Inert Gas Mixtures Through Highly Selective and Highly Permeable Polymer Membranes. *J. Membr. Sci.* **2005**, *251* (1–2), 29–41.

(32) Sun, L. Y.; Boo, W. J.; Clearfield, A.; Sue, H. J.; Pham, H. Q. Barrier Properties of Model Epoxy Nanocomposites. *J. Membr. Sci.* **2008**, *318* (1–2), 129–136.

(33) Gong, B.; Peng, Q.; Parsons, G. N. Conformal Organic–Inorganic Hybrid Network Polymer Thin Films by Molecular Layer Deposition using Trimethylaluminum and Glycidol. *J. Phys. Chem. B* **2011**, *115* (37), 11028–11028.